Draft Statistical Note: trends in surface displacements from InSAR following reduction in gas production

Stijn Bierman (Shell Global Solutions NL) and Rakesh Paleja (Shell Global Solutions UK)

October 29, 2015

Abstract

Since January 2014 , gas production at a number of wells near the town of Loppersum has been greatly reduced. In this progress note, we present methodology that may be used to assess whether or not there is evidence that the rate of surface displacements has decreased since this reduction in gas production on the basis of measurements made by Interferometric Synthetic Aperture Radar (InSAR). The InSAR data are in the form of estimated displacements in the Line-Of-Sight (dLOS) to the satellite between successive passes of the satellite for a number of locations at the surface which have been identified as Persistent Scatterers (PSs) or Distributed Scatterers (DSs).

The methodology is illustrated using time series of deformation estimates from the Terrasar-X (TSX) satellite in descending orbit from December 2011 to July 2015 (processing of the data was done by Skygeo (http://www.skygeo.com/); van den Heuvel and Schouten [2015]). We investigate trends in surface displacement rates of PSs and DSs in a radius of 250 meter of three permanent GPS stations (near the towns of Ten Post, Stedum and Zeerijp) in the area which may have been impacted by the changes in gas production. Two separate analyses have been presented of trends in displacement rates as apparent from global navigation satellite system data at these three GPS stations. In one of these studies it was concluded that, while there was evidence of continued subsidence in the area of the wells where production was reduced, evidence was also found that the rate of subsidence was lower in the area with reduced gas production relative to other areas after around mid-March or very early in April 2014 (Pijpers [2014] and Pijpers and van der Laan [2015]). In the other study it was reported that the rate of subsidence at the Ten Post station appears to be gradually decreasing, but no statistical confidence statements were made since it was concluded that more work was required to develop a suitable error model (van der Marel [2015]).

The InSAR data provide an alternative opportunity (next to GPS) to study displacement rates in relation to the production changes. The InSAR data provide better spatio-temporal coverage, which is valuable given that the inferences from GPS data in the above mentioned reports rely heavily on the data from the Ten Post station (since it is the only station in the potentially impacted area which was operational before 01-01-2014). There are also potential disadvantages to using PS and DS InSAR data. Separation of estimates of real deformation and potential atmospheric effects is required, and this may induce spatio-temporally correlated errors over both small and large (tens of kilometers) spatial and temporal scales. For both GPS and InSAR data, the major challenge is to separate different potential causes of surface deformation. Apparent surface displacements may be due to a combination of deep mass displacements such as reservoir compaction, shallow mass displacements and structural instabilities of the GPS monument or of the object creating the back-scatter. Potential problems caused by structural instabilities and multipath effects are in practice better manageable with GPS receivers since the monuments for mounting GPS receivers can be carefully chosen and designed such that potential problems are minimised. Instead, the PSs and DSs will be associated with a variety of objects with a likewise variety of potential structural instabilities. On the other hand, the spatial average (or median) of InSAR is more robust than the individual PS, whereas it is hard to validate if a GPS receiver is disturbed by local effects.

No evidence could be found in the InSAR data of trend changes in displacement rates following the production changes after January 2014. Instead, the displacement rates at the various locations could be described by a single linear trend. A visual comparison of GPS and InSAR displacements suggests that, in particular at the Ten Post location, there are some differences in the time trends suggested by both methods. We suggest that it is valuable to keep track of the GPS and InSAR trends at these locations and to get more insight into apparent discrepancies. More insight into this matter will develop as longer time series become available. There are many uncertainties involved in time series of surface displacements as measured by GPS, including the possibility of the presence of correlated errors in space and time (Williams [2015]). GPS as a technology for measuring surface displacements has been around for longer than PS and DS InSAR, and there is still some debate surrounding best practice for quantifying uncertainties in GPS measurements. Methods for errors in InSAR data are less well developed than those for GPS. The presented methodology

may be applied to other data sets from other satellites (or the same satellite in different orbits) and may be extended to cover a larger number of locations. We note that in this Draft Statistical Note not all avenues for analysing the PS and DS InSAR data have been explored. Questions remain regarding the best use and interpretation of the PS and DS InSAR data. In particular, we have refrained from applying formal statistical tests since more insight into the errors and error structure of the measured dLOS displacements is required.

Contents

1 Introduction

The load of the sediments above the gas bearing Rotliegend sandstone formation of the Groningen gas field is supported partially by the rock matrix itself and partially by the pressurized fluid and gas within the pore space of the rock. The decrease in fluid volume in the rock associated with gas extraction results in pore volume reduction (compaction) at the reservoir level. Compaction of the reservoir results in a measurable amount of ground displacements at the surface, and likely plays a role in inducing fault slip (NAM [2013]).

Since January 2014, gas production at a number of wells near the town of Loppersum has been greatly reduced. In this report statistical methodology is presented that may be used to assess whether or not the rate of surface displacements has changed since this reduction in gas production, using Interferometric Synthetic Aperture Radar (InSAR) measurements. The InSAR data have been preprocessed and are in the form of estimated displacements in the Line-Of-Sight (dLOS) to the satellite between successive passes of the satellite for a number of locations at the surface which have been identified as Persistent Scatterers (PSs) or Distributed Scatterers (DSs). These PSs and DSs are associated with features (e.g. buildings, roads, dikes) in the landscape from which the InSAR signal bounces back to the satellite and, taken over a number of successive passes of the satellite, resulted in a spatio-temporally interpretable signal.

The methodology is illustrated using time series of deformation estimates from the Terrasar-X (TSX) satellite in descending orbit from December 2011 to July 2015 (processing of the data was done by (processing of the data was done by Skygeo (http://www.skygeo.com/); van den Heuvel and Schouten [2015]), with one pass of the satellite every 11 days (TSX descending orbit 2 in table 1). Data from different orbits from the same satellite and from other satellites were available as well, but the data from TSX desc02 are likely to be the most suitable for detecting a change in surface displacement rates since these cover both a relatively long period before (55 passes of the satellite) and after (38 after passes) January 2014. We investigate trends in time series of PSs and DSs within a radius of 250 meter of one of three permanent GPS stations (near the towns of Ten Post, Stedum and Zeerijp) which fall within the area in which surface displacement rates may have been impacted by the changes in gas production. The GPS receivers at Zeerijp and Stedum became operational in April 2014, after the changes in production had taken place. The GPS receiver at Ten Post became operational in March 2013 and thus provides information on displacements both before and after the production change. Analyses of trends in displacement rates at these three GPS stations, measured using global navigation satellite system (GNSS) data, have been presented in three reports (Pijpers [2014]; Pijpers and van der Laan [2015]; van der Marel [2015]). In a series of two reports from Statistics Netherlands it was concluded that, while there was evidence of continued subsidence in the area of the wells where production was reduced, evidence was also found that the rate of subsidence was lower in the area with reduced gas production relative to other areas after around mid-March or very early in April 2014 (Pijpers [2014] and Pijpers and van der Laan [2015]). In the third report, from Delft Technical University (van der Marel [2015]), it was reported that the rate of subsidence at the Ten Post station appears to be gradually decreasing, but no statistical confidence statements were made since it was concluded that more work was required to develop a suitable error model.

The InSAR data provide an alternative opportunity (next to GPS) to study displacement rates in relation to the production changes. Potential advantages of the PS and DS InSAR data over the GPS data are that the InSAR data provides information on displacement rates both for a period before and after the production changes at a much larger set of locations. However, we note that there are also potential disadvantages to using PS and DS InSAR data. In general, more assumptions have to be made to interpret InSAR data compared to GPS. Separation of estimates of real deformation and potential atmospheric effects is required, and detailed knowledge of atmospheric conditions is necessary for this purpose. This may induce spatio-temporally correlated errors over both small and large (tens of kilometers) spatial and temporal scales. Estimates of displacements from both GPS and InSAR may be affected by multipath effects caused by the reflection of signals from neighbouring terrain. For both GPS and InSAR data, the major challenge is to separate different causes of surface deformation. Apparent surface displacements may be due to a combination of deep mass displacements such as reservoir compaction, shallow mass displacements (e.g. due to changes in ground water level, or shallow compaction) and structural instabilities of the GPS monument or of the object creating the back-scatter. However potential problems caused by structural instabilities and multipath effects are in practice better manageable with GPS receivers since the monuments for mounting GPS receivers can be carefully chosen and designed such that potential problems are minimised. Instead, the PSs and DSs will be associated with a variety of objects with a likewise variety of potential structural instabilities, and in practice this is difficult to take into account in the analysis of these data. On the other hand, the spatial average (or median) of InSAR is more robust than the individual PS, whereas it is hard to validate if a GPS receiver is disturbed by local effects. We note that SAR images provide only information on relative displacements in the line-of-sight to the satellite. In the processing of the TSX data, estimates of absolute line-of-sight displacements have been obtained through a reference based on a mix of GPS rates and stable areas. It is possible that some errors may be induced by the estimation of the reference.

Table 1: Available InSAR data for a number of satellites, with their associated orbit and average geodetic azimuth (α) and incidence angle (θ). The angles are in degrees. In this report, data from the TSX satellite in descending orbit 2 have been used (row with text in bold font).

Name	Orbit	start	end	frequency	α	θ
TSX	descending orbit 1	Jun 2013	July 2015	11 days	102.0	26.2
TSX	**descending orbit 2**	**Dec 2011**	**July 2015**	**11 days**	**100.5**	**37.3**
TSX	ascending orbit	Jun 2013	July 2015	11 days	258.6	31.0
Radarsat	descending orbit	Sep 2009	Jun 2015	24 days	100.3	33.9
Envisat	descending orbit	Dec 2003	Sep 2010	35 days	102.4	23.0
Envisat	ascending orbit	Jun 2006	Aug 2010	35 days	255.7	23.0

2 Permanent GPS stations in the area of interest

In this report, PS and DS InSAR time series that fall within in a radius of 250 meters of one of three permanent GPS stations (Ten Post, Stedum and Zeerijp) have been used in the statistical analyses (Figure 1). The GPS stations at Stedum and Zeerijp have been attached to specially constructed monuments with a foundation of more than 20 meters deep. The GPS receiver at Ten Post has been mounted to a metal red which is attached to the wall of a building. For illustration, pictures of the three permanent GPS stations are given in an Appendix to this report (Figure 18).

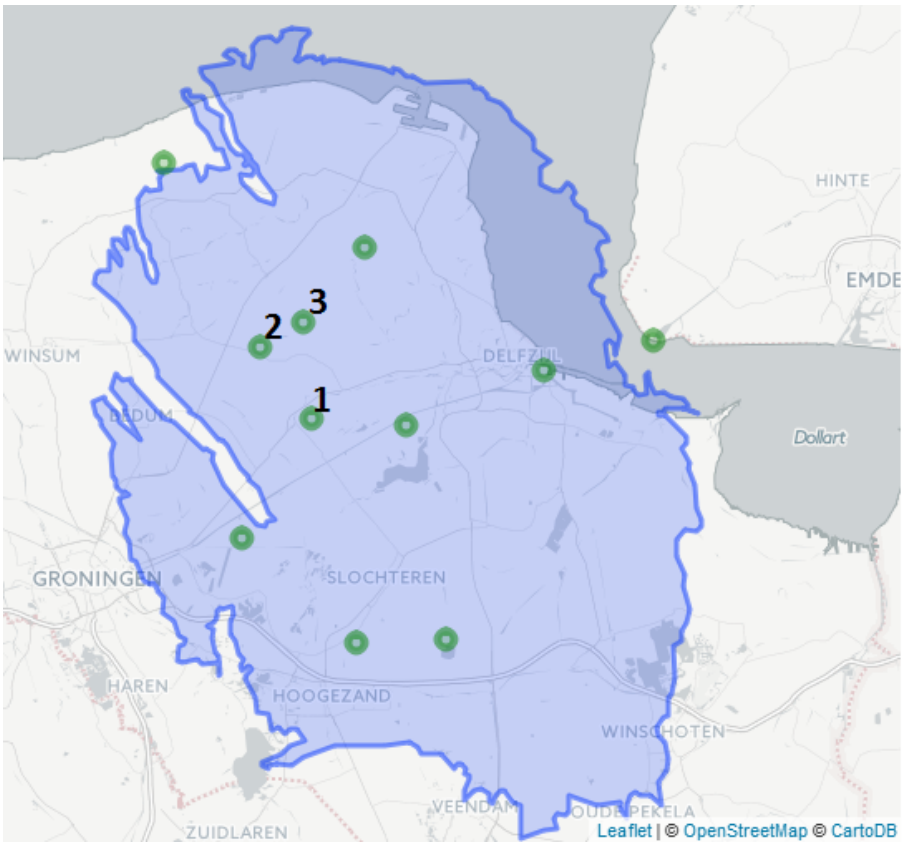

Figure 1: A map of the North-East of the Netherlands, with an outline of the Groningen gas field (blue polygon) and locations of permanent GPS stations (green circles). In this report, PS and DS InSAR time series that fall within in a radius of 250 meters of one of three permanent GPS stations (1: Ten Post, 2: Stedum, 3: Zeerijp) have been used for analyses of trends in surface displacements.

Maps of the PS and DS InSAR locations for the three locations are given in Appendix A. At the Ten Post location, within a radius of 250 m of the GPS receiver, there were 2587 PS and DS locations (Figure 14). At the Stedum location, within a radius of 250 m of the GPS receiver, there were 256 PS and DS locations (Figure 13). At the Zeerijp location, within a radius of 250 m of the GPS receiver, there were 47 PS and DS locations (Figure 15).

3 Conventions

We use the following conventions for displacements and angles:

- Displacement in the line of sight to the satellite, dLOS, towards the satellite is positive.
- Displacement from west to east, dx, is positive.
- Displacement from south to north, dy, is positive.
- The geodetic azimuth, α, is defined in degrees clockwise from polar north.
- The incidence angle, θ, is defined with respect to the vertical (z).

Given these conventions, a unit displacement in the horizontal (dx and dy) and vertical (dz) at a surface location will result in dLOS units displacement in the line of sight to the satellite, where:

$$dLOS = dh\ \sin(\theta) + dz\ \cos(\theta) \tag{1}$$

$$dh = dx\ \sin(\alpha) + dy\ \cos(\alpha) \tag{2}$$

An illustration of the conventions used for the angles and displacements is given in figure 2.

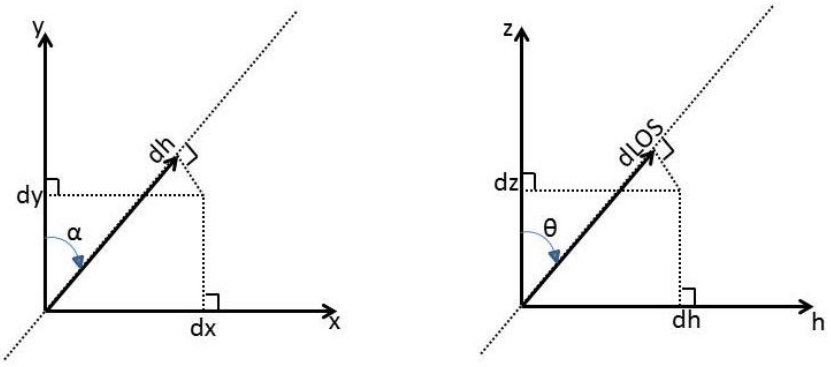

Figure 2: Illustration of the conventions used to compute displacements in line-of-sight to the satellite (dLOS).

The same conventions have been adhered to for transforming the displacements in the horizontal and vertical directions from GPS data to line-of-sight displacements.

4 Data visualisations

Let $y_{i,dt}$ be the dLOS at location (persistent scatterer or distributed scatterer) i over the time interval dt. The type of scatterer associated with location i is denoted by $k(i) \in \{\text{PS}, \text{DS}\}$. The TSX satellite takes 11 days to orbit the earth. This means that in principle a measurement is available every 11 days. However, in some cases one or more (up to four) measurements were not available. Three different time series of dLOS per location were constructed:

- "Baselining": All measurements were differenced with respect to the first observation (2011-12-14). Using this approach, the first measurement in the time series is the dLOS associated with the time interval between the following two consecutive passes of the satellite: 2011-12-14 and 2011-12-25. The last measurement in the time series is the dLOS associated with the time interval 2011-12-14 - 2015-07-26. This meant that, for each location, a time series was available of 93 dLOS measurements from 2011-12-25 through to 2015-07-26.
- "Before period": All measurements were differenced with respect to the first observation (2011-12-14), but only measurements up to and including December 2013 were used. Using this approach, the first measurement in the time series is the dLOS associated with the time interval between the following two consecutive passes of the satellite: 2011-12-14 and 2011-12-25. The last measurement in this time series is the dLOS associated with the time interval 2011-12-14 - 2013-12-31. This meant that, for each location, a time series was available of 55 dLOS measurements from 2011-12-25 through to 2013-12-31.
- "After period": All measurements that were made after 2013-12-31 were differenced with respect to the measurement from 2013-12-31. Using this approach, the first measurement in the time series is the dLOS associated with the time interval between the following two consecutive passes of the satellite: 2013-12-31 and 2014-02-02. The last measurement in this time series is the dLOS associated with the time interval 2013-12-31 - 2015-07-26. This meant that, for each location, a time series was available of 38 dLOS measurements from 2014-02-02 through to 2015-07-26.

Surface displacements due to reservoir compaction are expected to vary little over short distances, given the burial depth of approximately 3000 meters subsurface of the reservoir. However, visual inspection of the time series data indicated that, even over short distances, there can be considerable variability in dLOS measurements. The minimum and maximum dLOS at each pass of the satellite can vary widely between locations (Figure 16), and part of this variability may be due to phase ambiguities. The wavelength of the TSX satellite is 3.1 cm (X-band), and most (if any) phase ambiguities can be expected to be half of the wavelength because of the 2-way travel of the signal (satellite-ground-satellite). The median and the 10%-iles and 90%-iles of the ranked dLOS measurements for each pass of the satellite are given in Figure 3. The 10%-iles and 90%-iles of the ranked dLOS measurements vary considerably less than the minimum and maximum, indicating that the distribution ("spread") of the dLOS measurements at each epoch is "heavy-tailed". The broad trend in surface displacements due to reservoir compaction is apparent in nearly all of the individual time series and in the time series of the median dLOS. Visual inspection suggests that a good first order description of the trends over time appear is to assume that these are linear and time-invariant, although perhaps with a seasonal trend. Examples of time series and fitted trend models are given in figure 4 for four time series from the Ten Post location. Part of the variability in dLOS between locations is likely to be associated with the type of object at the surface which is creating the interpretable backscatter to the satellite. We note therefore that a thorough analysis of these data would involve a detailed analysis of the relationship between trend in displacements and the type and characteristics of the object. However, in practice this is difficult to achieve, and in this report we have limited ourselves to investigating potential differences between PSs and DSs on displacement rates. There was no strong evidence to suggest that type of scatterer could be used to explain the variability in signals (Figure 16, 17 and Figure 3).

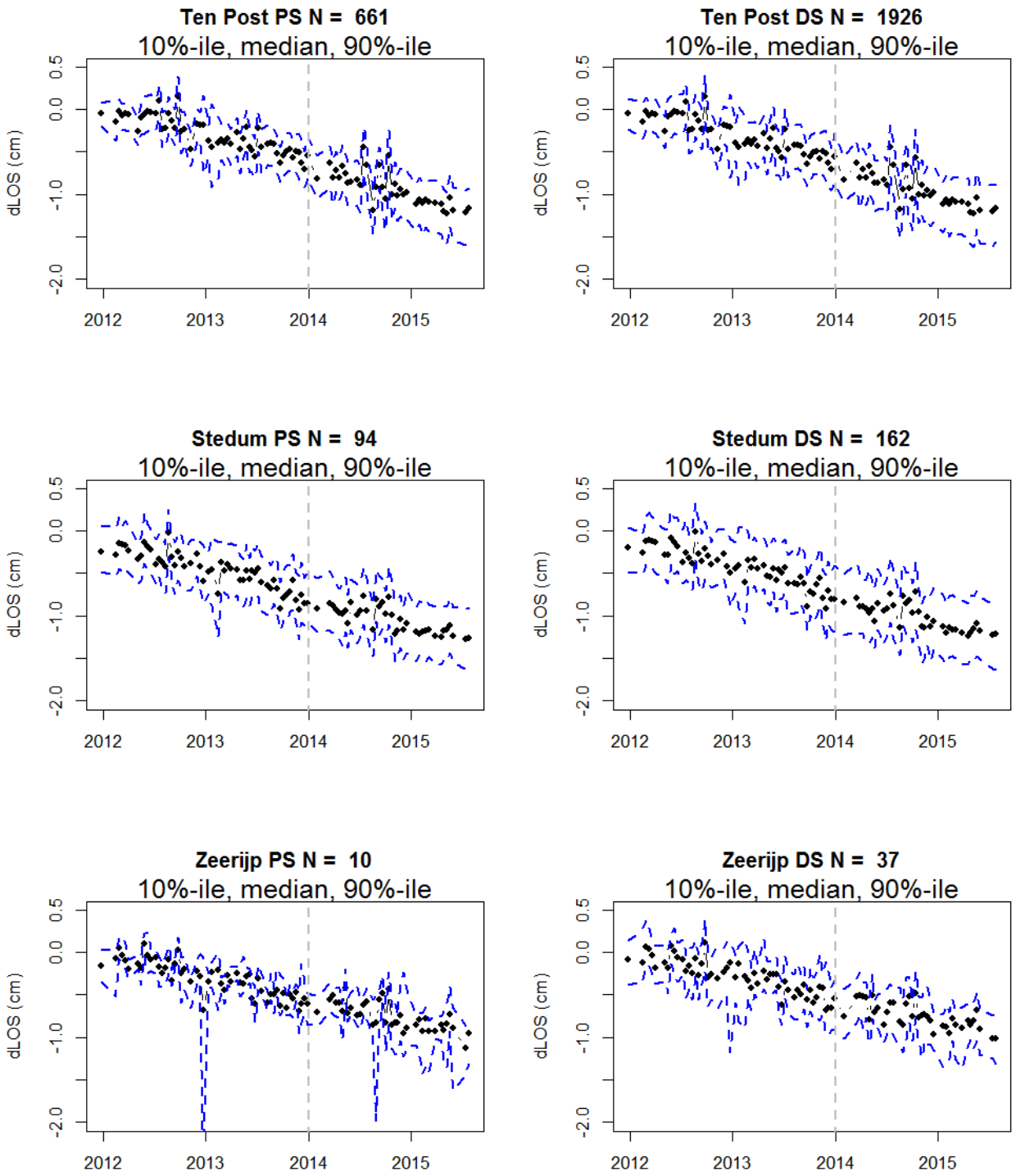

Figure 3: The median (50%-ile; filled dots) values and the values associated with the 10%-ile and 90%-ile (grey dashed lines) of the ranked dLOS measurements for PS and DS scatterers per location.

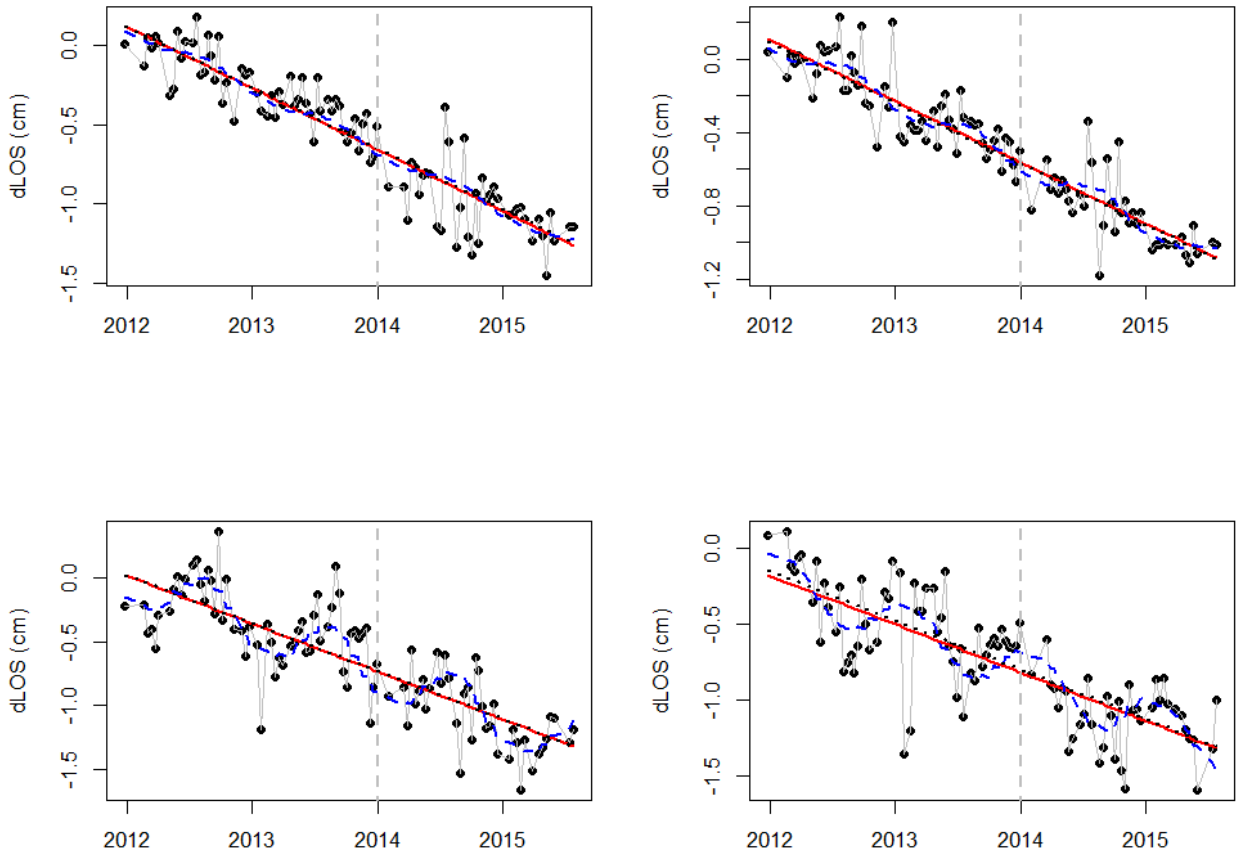

Figure 4: Examples of dLOS time series associated with four persistent back-scatterers from the Ten Post location. The filled dots (connected by grey lines) give the measured dLOS. The straight red lines indicate the linear trend in displacement rate as estimated using Ordinary Least Squares (OLS; model 3). The straight dotted black lines indicate the robust estimate of the linear trend in displacement rate (see text). We note that the robust and OLS estimates are in most cases highly similar and difficult to distinguish from one another. The blue lines indicate the fitted trend of the model with seasonality (model 4)

.

For each location i, we estimated the average displacement rate b_i per time series ("Complete time series", "Before period" and "After period") by fitting a linear trend with time. All models were implemented using the R language for statistical computing (R Core Team [2014]). The linear trend was estimated in three different ways:

Model 1 (Equation 3), in which b_i^{OLS} was estimated using Ordinary Least Squares (OLS). In this model, we assume linearity, homoscedasticity, and uncorrelated errors:

$$y_{i,dt} = a_i^{OLS} + b_i^{OLS} T(dt) + e_{i,dt} \tag{3}$$

Where a_i^{OLS} is an intercept, $e_{i,dt}$ the model residuals, and $T(dt)$ the length of time (number of days) associated with the interval dt. We note that we express estimates of b_i in cm/year. The conversion from day to year is done by multiplying the estimates of b_i by 365.25.

Model 2: A robust linear trend estimate of b_i^{Rob}, estimated using the same linear trend model as decribed above (Equation 3), but instead of minimizing the sum of squared residuals, a robust estimator (M-estimator) was used which minimizes the sum of a less rapidly (compared to squaring of errors) increasing function of the residuals (see e.g. F. R. Hampel and Stahel [1986]). For this method, an iterative procedure (iteratively

reweighted least squares) is necessary. This model was implemented using the functionality for robust trend estimation in the "MASS" package in R (the "rlm" function in Venables and Ripley [2002]).

Model 3 (Equation 4): A model with seasonality in displacement rates in which b_i^S was estimated using Ordinary Least Squares (OLS) together with a smooth function for calendar month to represent potential seasonal variability:

$$y_{i,dt} = a_i^S + b_i^S T(dt) + s(m_{(dt)}) + e_{i,dt} \quad (4)$$

Where $s(m_{(dt)})$ is a smooth function represented using penalized regression splines. The spline bases in this analysis are cyclic, which means that only smooth transitions are allowed between all months, including the months of December and January. The amount of smoothness is estimated using generalised cross-validation. This model is implemented using the functionality for generalised additive modeling (gam; see e.g. Hastie and Tibshirani [1990]) in R (Wood [2006], Wood [2011]). The potential flexibility of the fitted curve for the seasonal response is governed partly by the basis dimension. The basis dimension (the number of knots at which the spline is allowed to "flex") should be large enough to allow for enough flexibility to fit the potential shapes of the seasonal curves that may reasonably be expected. Here, we have chosen to fit the models using 12 knots, equal to the number of calendar months. The actual degrees of freedom of the models are estimated using cross-validation, and were in all cases much less than 12, which indicates that the number of knots was not restricting the shape of the seasonal curves that were fitted.

We note that, due to the imposed smooth transition between December and January, the trend estimates of b_i^S and b_i^{OLS} are identical. The choice of method for estimating the linear trend was of little consequence, since there was good correspondence between b_i^{Rob} and b_i^{OLS} (Figure 5).

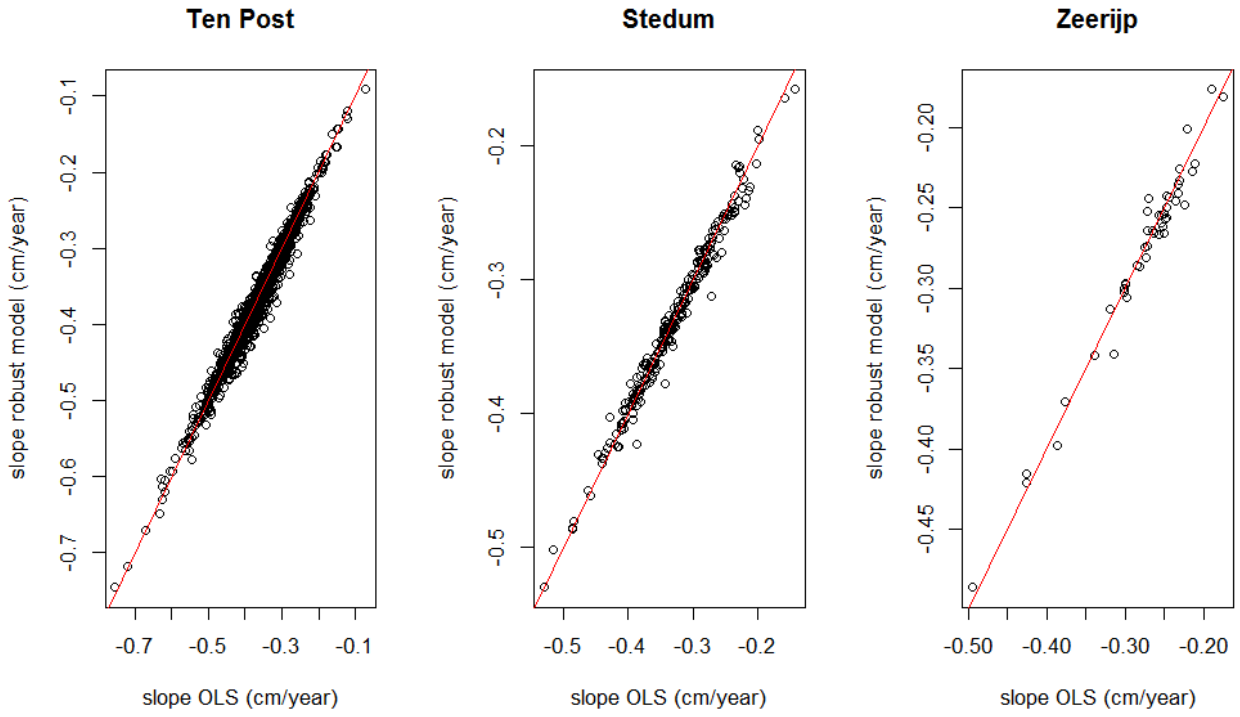

Figure 5: Comparison of trends in displacement rate, estimated using either Ordinary Least Squares (OLS; model 3) or a robust method (see text).

Examples of time series and fitted trend models are given in figure 4 for four time series from the Ten Post location. For some locations, it is obvious that there is seasonality in the signal. Maps which depict the variability in estimated trends and amplitudes of the PS and DS InSAR locations for the three locations are given in Appendix A and B.

We note that there appears to be a reasonable agreement between the signals from GPS and the median dLOS from InSAR for the Zeerijp and Stedum locations, but not for the Ten Post location (Figure 19). The reasons for the apparent discrepancy in signals from InSAR and GPS at the Ten Post location is unclear.

5 Results

For each of the three locations, an overview of results of the estimated linear trends in surface displacements in the before and after periods is given (Figure 6). The estimates of average displacement rates in both periods were differenced (per PS or DS location) to get an estimate of the potential trend change. At some locations there was a higher displacement rate, and at others a lower displacement rate, in the "after" period compared to the "before" period (Figure 6). Thus, there appears to be little evidence of a consistent shift in displacement rates between the two period.

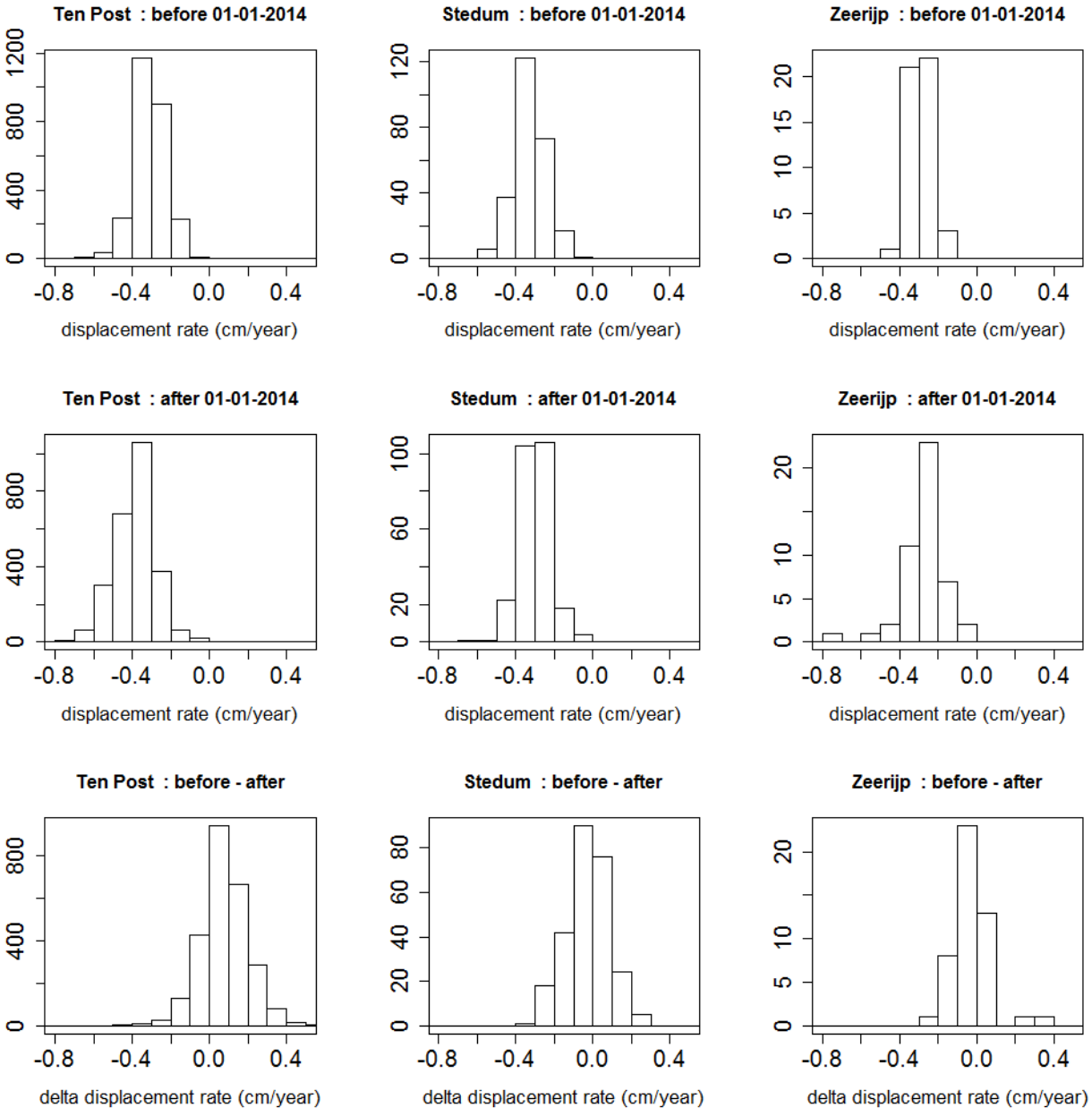

Figure 6: An overview, for each of the three locations, of the estimated linear trends in surface displacements in the "before" (top three panels) and "after" (three panels in the middle row) periods, and the difference between the estimated trends for both periods per location (bottom three panels).

Time series of median displacements for each of the three locations, and fitted linear trends, are given in figures 7 8 and 9. Visual inspection of these time series indicates that the displacement rates can be reasonably described by a time-invariant linear trend. A scatterplot smoother of the model residuals does

not reveal trends in residuals over time.

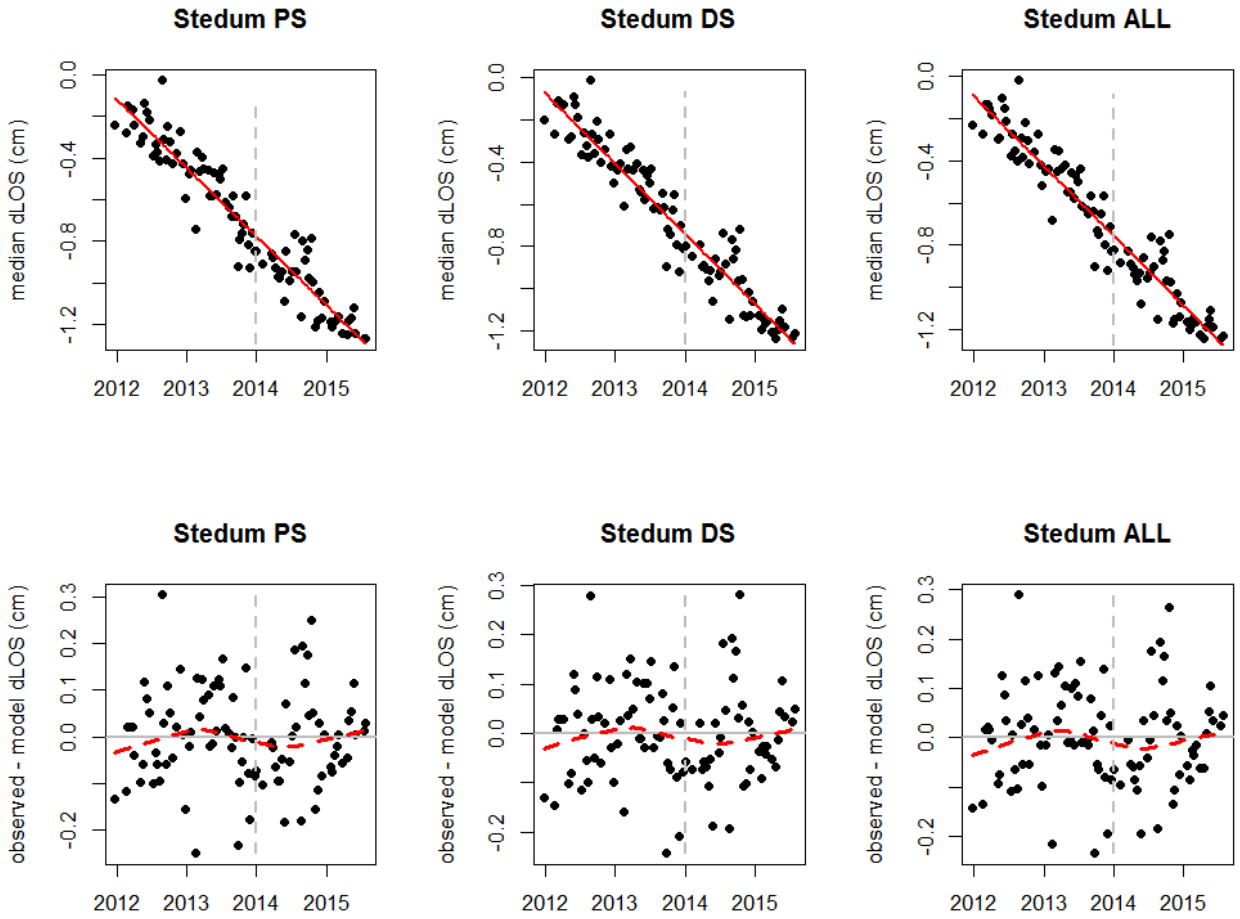

Figure 7: Stedum Location. Top row: Time series of median displacements (filled dots) with fitted linear trend (red line). Bottom row: model residuals with a scatter plot smoother for the average in residuals over time.

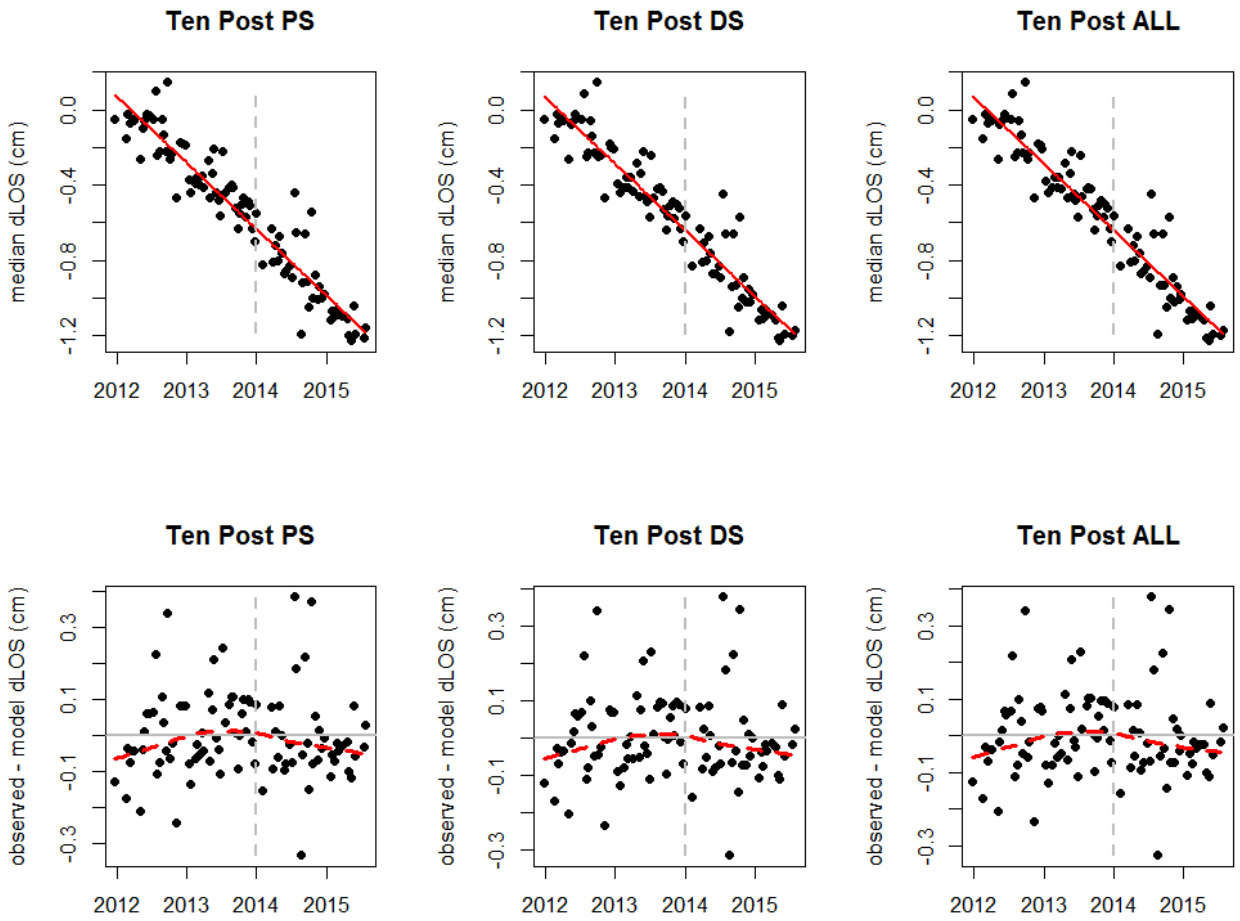

Figure 8: Ten Post Location. Top row: Time series of median displacements (filled dots) with fitted linear trend (red line). Bottom row: model residuals with a scatter plot smoother for the average in residuals over time.

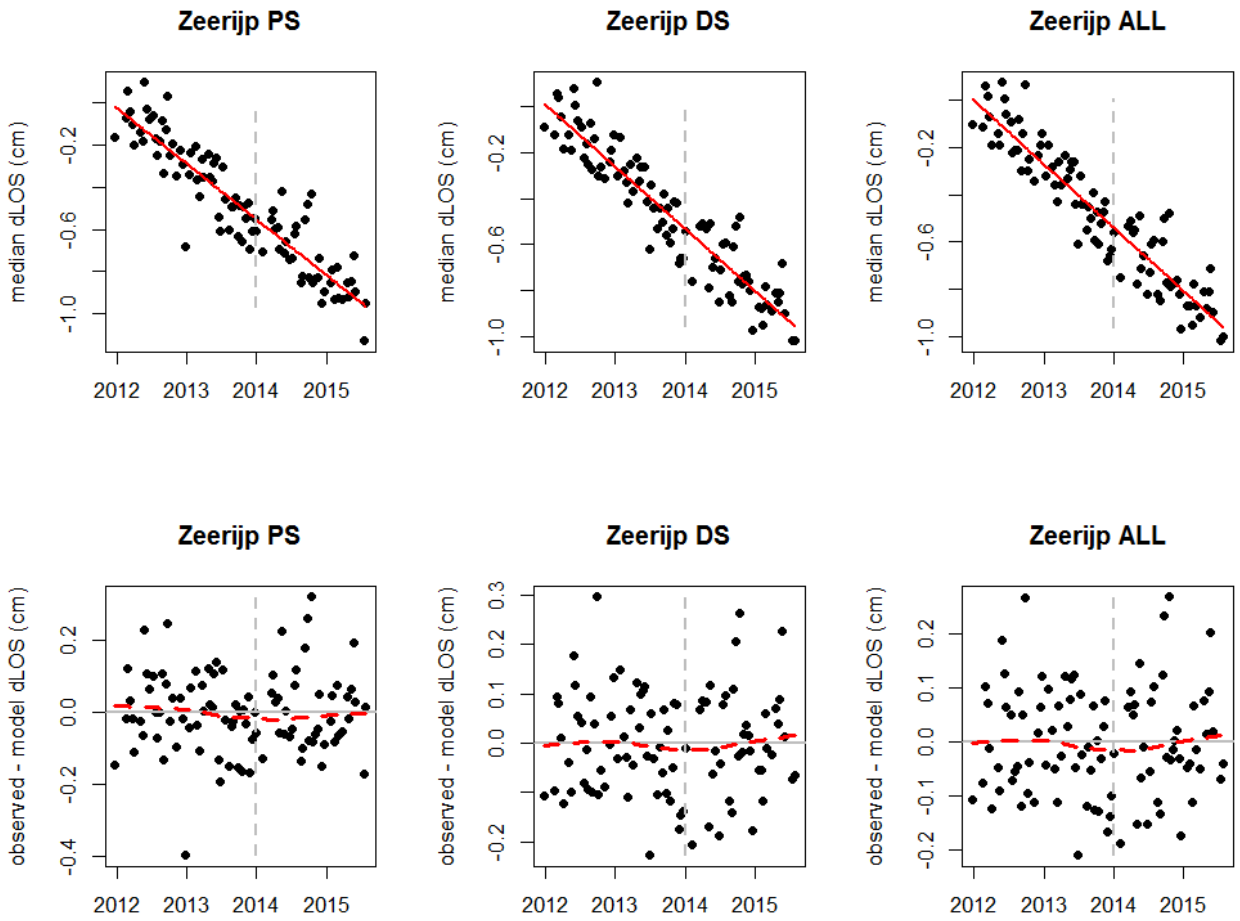

Figure 9: Zeerijp Location. Top row: Time series of median displacements (filled dots) with fitted linear trend (red line). Bottom row: model residuals with a scatter plot smoother for the average in residuals over time.

6 Discussion and Conclusions

Since January 2014 , gas production at a number of wells near the town of Loppersum has been greatly reduced. In this Draft Progress Note, we present methodology that may be used to assess whether or not there is evidence that the rate of surface displacements has decreased since this reduction in gas production on the basis of measurements made by Interferometric Synthetic Aperture Radar (InSAR). The InSAR data are in the form of estimated displacements in the Line-Of-Sight (dOS) to the satellite between successive passes of the satellite for a number of locations at the surface which have been identified as Persistent Scatterers (PSs) or Distributed Scatterers (DSs).

The methodology is illustrated using time series of deformation estimates from the Terrasar-X (TSX) satellite in descending orbit from December 2011 to July 2015 (processing of the data was done by Skygeo (http://www.skygeo.com/)). We investigate trends in surface displacement rates of PSs and DSs in a radius of 250 meter of three permanent GPS stations (near the towns of Ten Post, Stedum and Zeerijp) in the area which may have been impacted by the changes in gas production. Two separate analyses have been presented of trends in displacement rates as apparent from global navigation satellite system data at these three GPS stations. In one of these studies it was concluded that, while there was evidence of continued subsidence in the area of the wells where production was reduced, evidence was also found that the rate of subsidence was lower in the area with reduced gas production relative to other areas after around mid-March or very early in April 2014 (Pijpers [2014] and Pijpers and van der Laan [2015]). In the other study it was reported that the rate of subsidence at the Ten Post station appears to be gradually decreasing, but no statistical confidence statements were made since it was concluded that more work was required to develop a suitable error model (van der Marel [2015]).

The InSAR data provide an alternative opportunity (next to GPS) to study displacement rates in relation to the production changes. The InSAR data provide better spatio-temporal coverage, which is valuable given that the inferences from GPS data in the above mentioned reports rely heavily on the data from the Ten Post station (since it is the only station in the potentially impacted area which was operational before 01-01-2014). There are also potential disadvantages to using PS and DS InSAR data. Modeling assumptions are required to solve phase ambiguities. Separation of estimates of real deformation and potential atmospheric effects is required, and this may induce spatio-temporally correlated errors over both small and large (tens of kilometers) spatial and temporal scales. For both GPS and InSAR data, the major challenge is to separate different potential causes of surface deformation. Apparent surface displacements may be due to a combination of deep mass displacements such as reservoir compaction, shallow mass displacements and structural instabilities of the GPS monument or of the object creating the back-scatter. Potential problems caused by structural instabilities and multipath effects are in practice better manageable with GPS receivers since the monuments for mounting GPS receivers can be carefully chosen and designed such that potential problems are minimised. Instead, the PSs and DSs will be associated with a variety of objects with a likewise variety of potential structural instabilities. On the other hand, the spatial average (or median) of InSAR is more robust than the individual PS, whereas it is hard to validate if a GPS receiver is disturbed by local effects. We note that SAR images provide only information on relative displacements in the line-of-sight to the satellite. In the processing of the TSX data, estimates of absolute line-of-sight displacements have been obtained through a reference based on a mix of GPS rates and stable areas. It is possible that some errors may be induced by the estimation of the reference.

No evidence could be found in the InSAR data of trend changes in displacement rates following the production changes after January 2014. Instead, the displacement rates at the various locations could be described by a single linear trend. A visual comparison of GPS and InSAR displacements suggests that, in particular at the Ten Post location, there are some differences in the time trends suggested by both methods. We suggest that it is valuable to keep track of the GPS and InSAR trends at these locations and to get more insight into apparent discrepancies. More insight into this matter will develop as longer time series become available. There are many uncertainties involved in time series of surface displacements as measured by GPS, including the possibility of the presence of correlated errors in space and time (Williams [2015]). GPS as a technology for measuring surface displacements has been around for longer than PS and DS InSAR, and there is still some uncertainty surrounding best practice for appropriate methods for quantifying uncertainties in GPS measurements. Methods for errors in InSAR data are less well developed than those for GPS.The presented methodology may be applied to other data sets from other satellites (or the same satellite in different orbits) and may be extended to cover a larger number of locations. We note that in this Draft Statistical Note not all avenues for analysing the PS and DS InSAR data have been explored. Questions remain regarding the best use and interpretation of the PS and DS InSAR data. In particular, we have refrained from applying formal statistical tests since more insight into the errors and error structure of the measured dLOS displacements is required.

A Maps of distributed and persistent scatterers: estimated linear trends

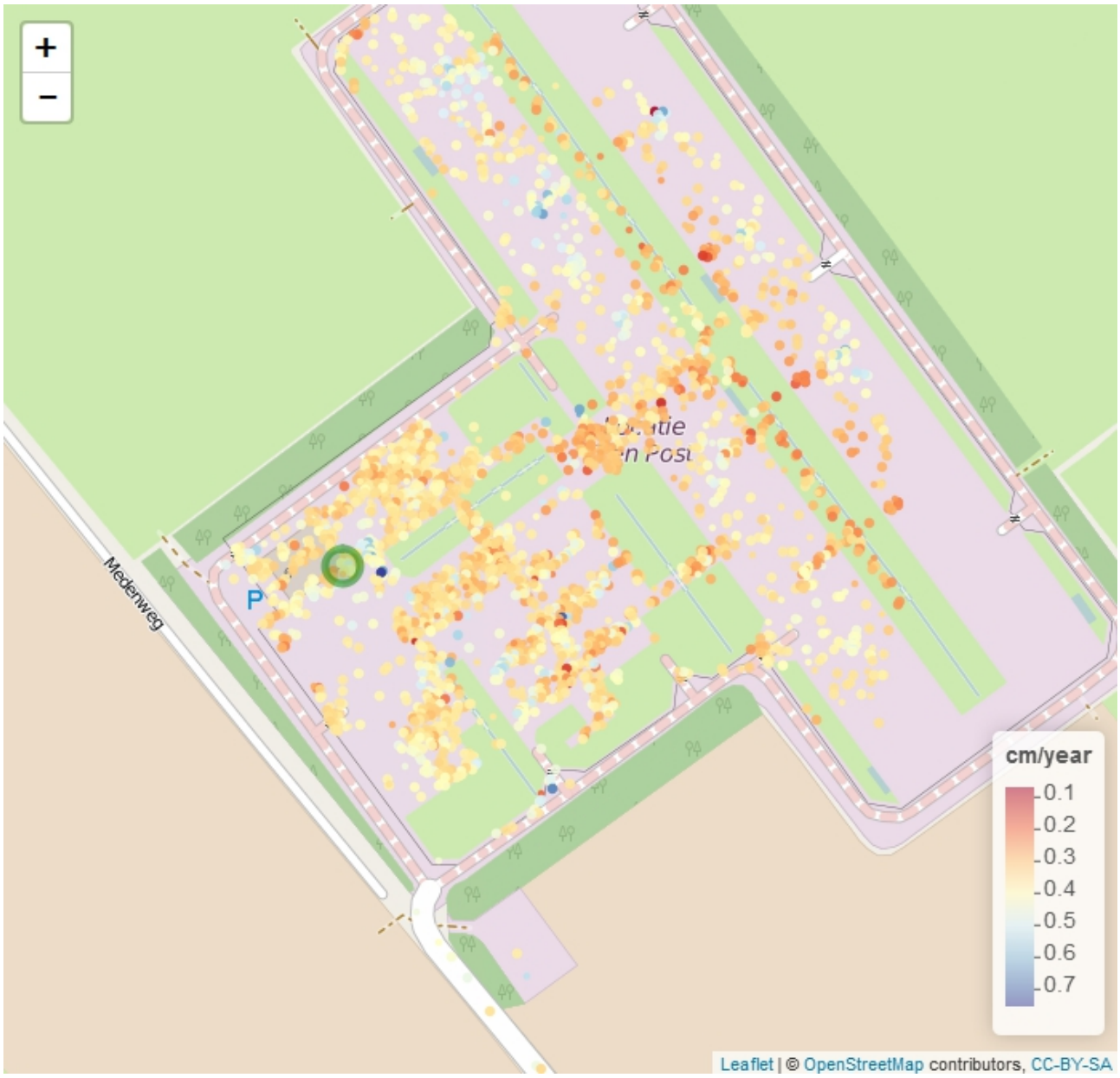

Figure 10: Ten Post: map of PS and DS InSAR locations with their associated estimates of average surface displacements in the line-of-sight (linear trend). The green circle indicates the location of the GPS receiver. PS and DS locations have been selected that fall within a radius of 250 meters of the GPS receiver.

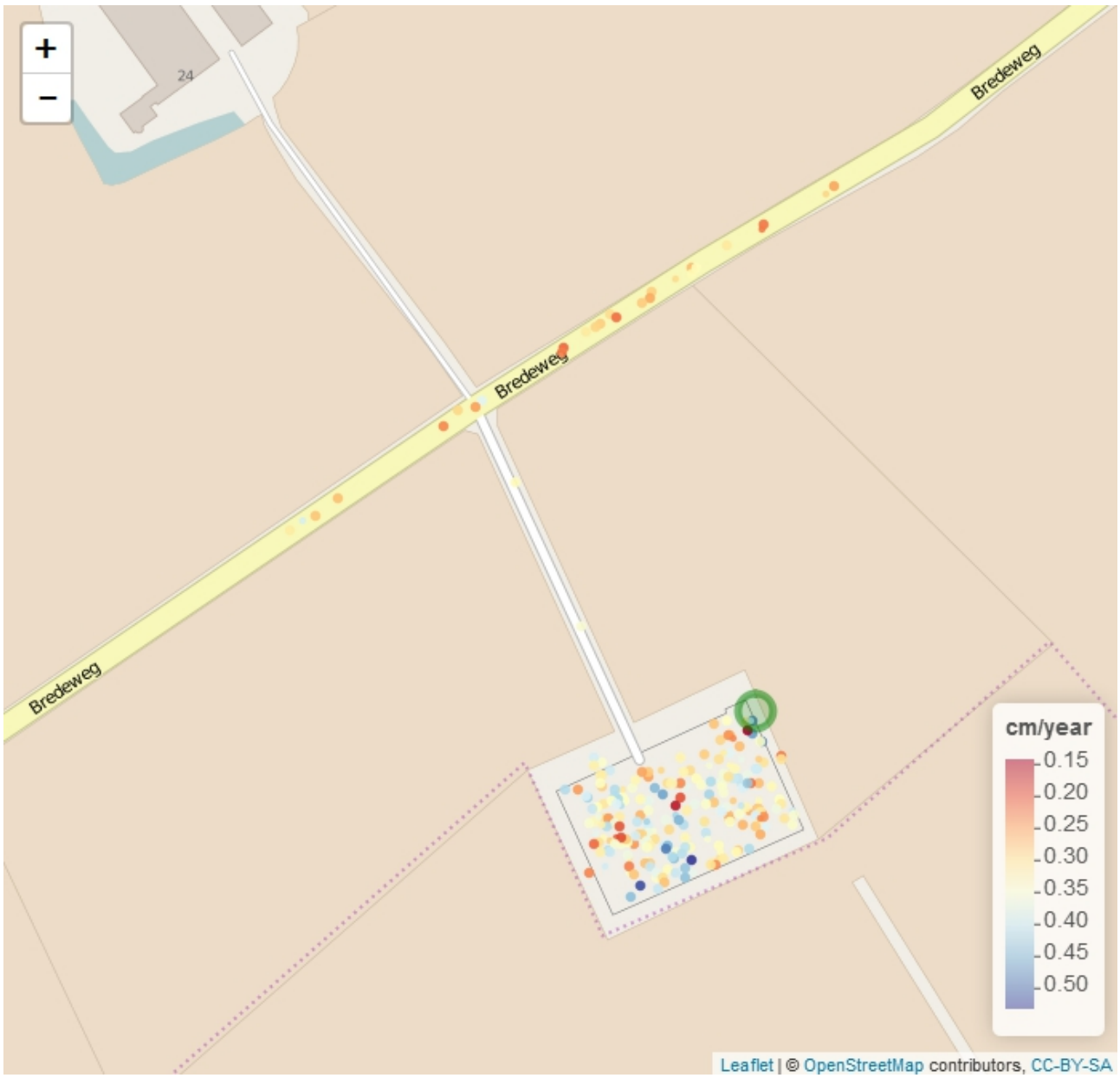

Figure 11: Stedum: map of PS and DS InSAR locations with their associated estimates of average surface displacements in the line-of-sight (linear trend). PS and DS locations have been selected that fall within a radius of 250 meters of the GPS receiver.

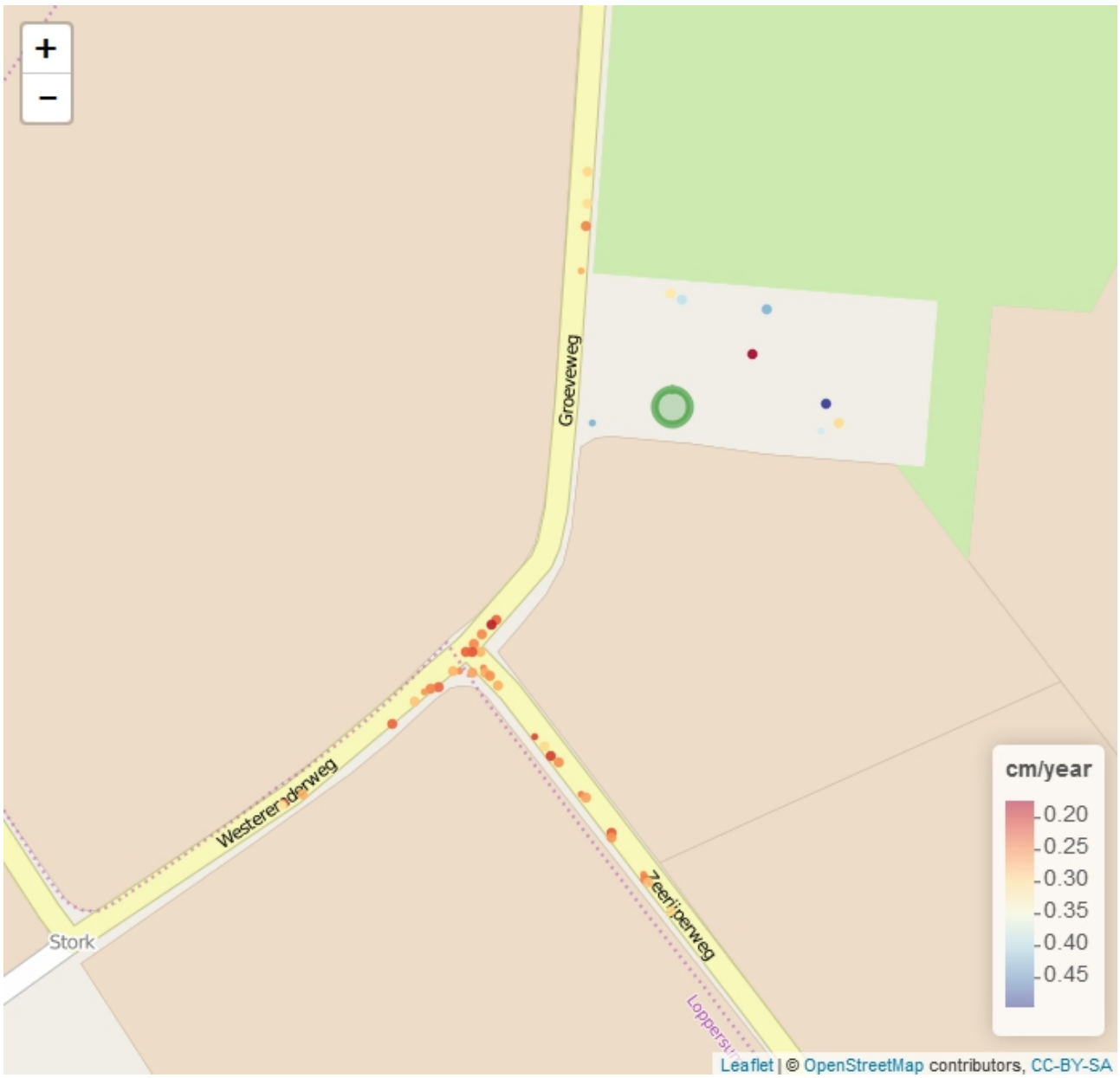

Figure 12: Zeerijp: map of PS and DS InSAR locations with their associated estimates of average surface displacements in the line-of-sight (linear trend). PS and DS locations have been selected that fall within a radius of 250 meters of the GPS receiver.

B Maps of distributed and persistent scatterers: estimated amplitudes

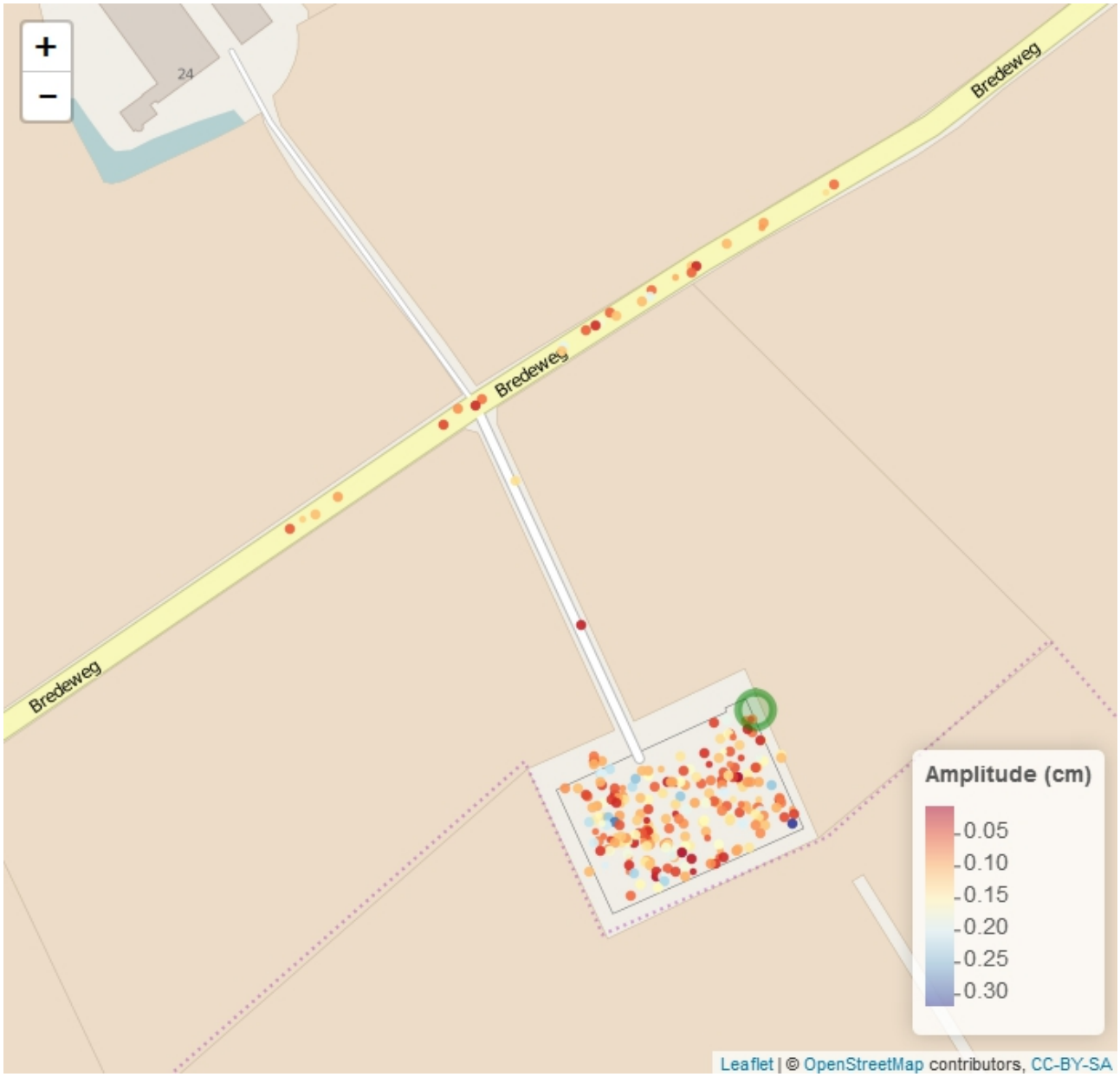

Figure 13: Stedum: map of PS and DS InSAR locations with their associated estimated amplitudes of the seasonal signal.

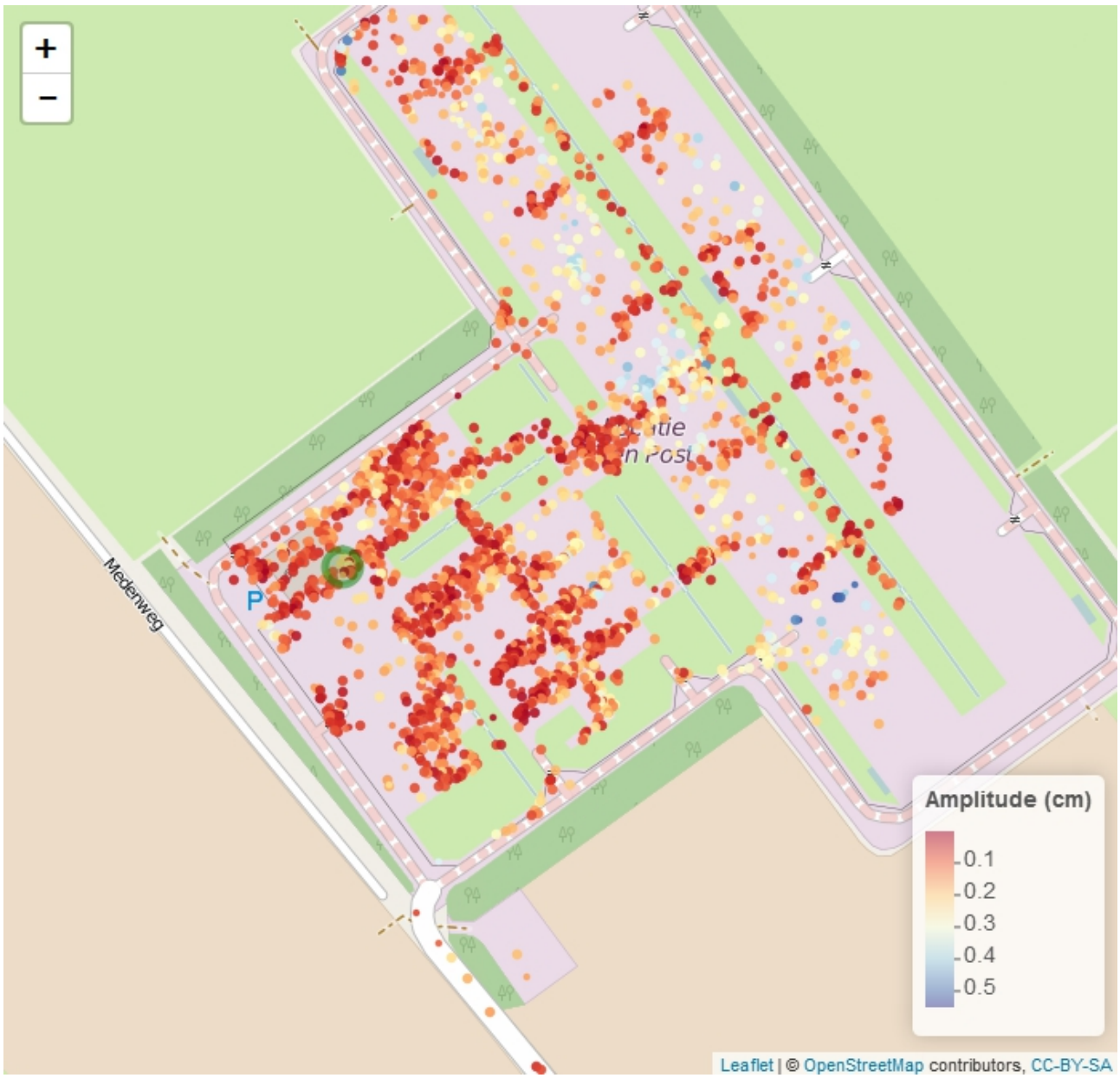

Figure 14: Ten Post: map of PS and DS InSAR locations with their associated estimated amplitudes of the seasonal signal.

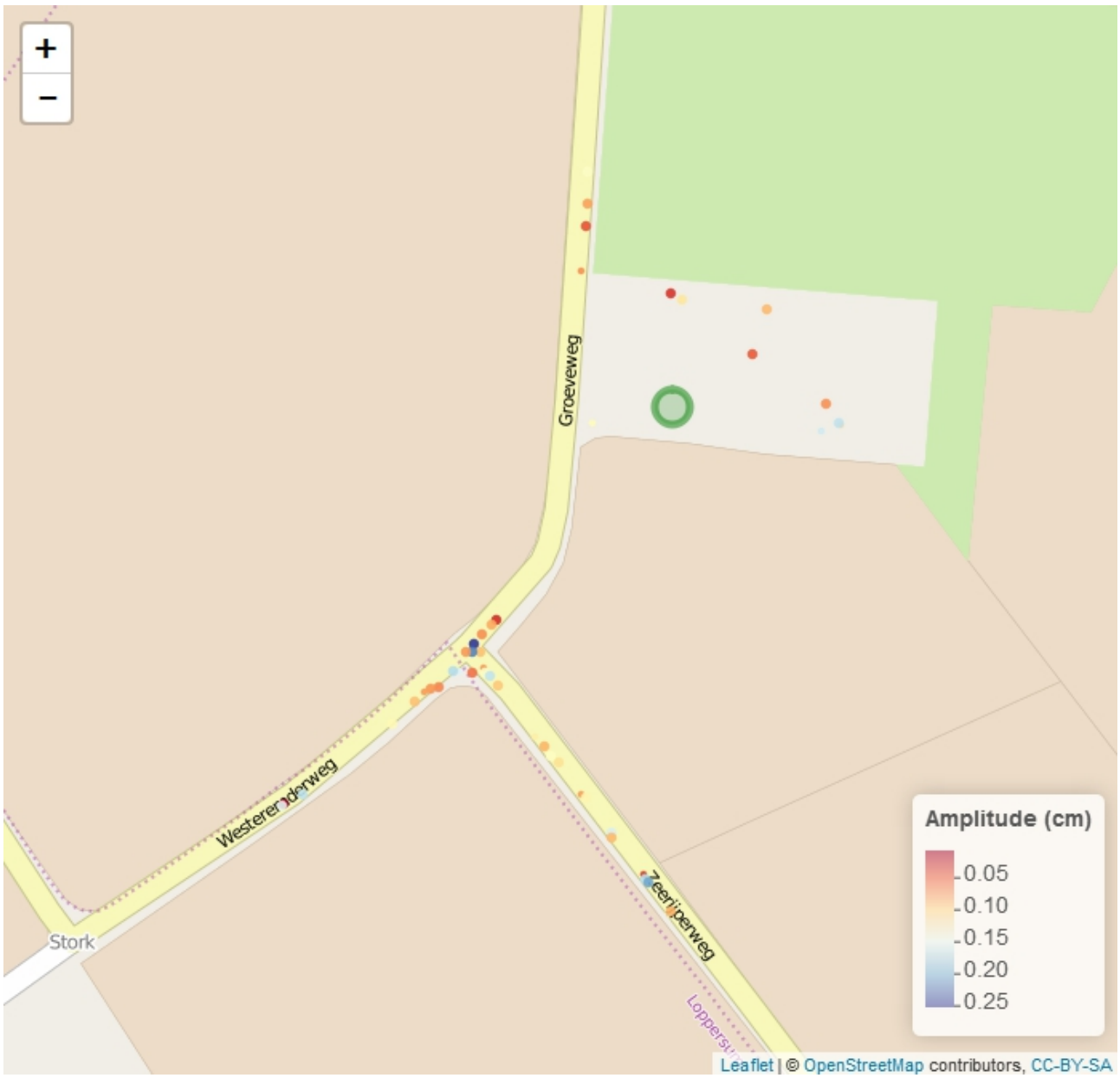

Figure 15: Zeerijp: map of PS and DS InSAR locations with their associated estimated amplitudes of the seasonal signal.

C Boxplots of spread in dLOS measurements PS and DS InSAR

In this report, we make use of boxplots (or "box-and-whisker" plots) to visualise the variability (distribution) of data or estimates of a particular variable, without making an assumption with respect tot the potential underlying statistical distribution of these data. We use the following definitions for constructing the boxplots (see e.g. Frigge et al. [1989]):

- The bottom and top of the box are the first and third quartiles
- The band inside the box is the second quartile (the median).
- The whiskers (if any) represent the lowest datum still within 1.5 times the Inter-Quartile range (IQR), and the highest datum still within 1.5 times the IQR of the upper quartile. The IQR is defined as the difference between the first and third quartiles.

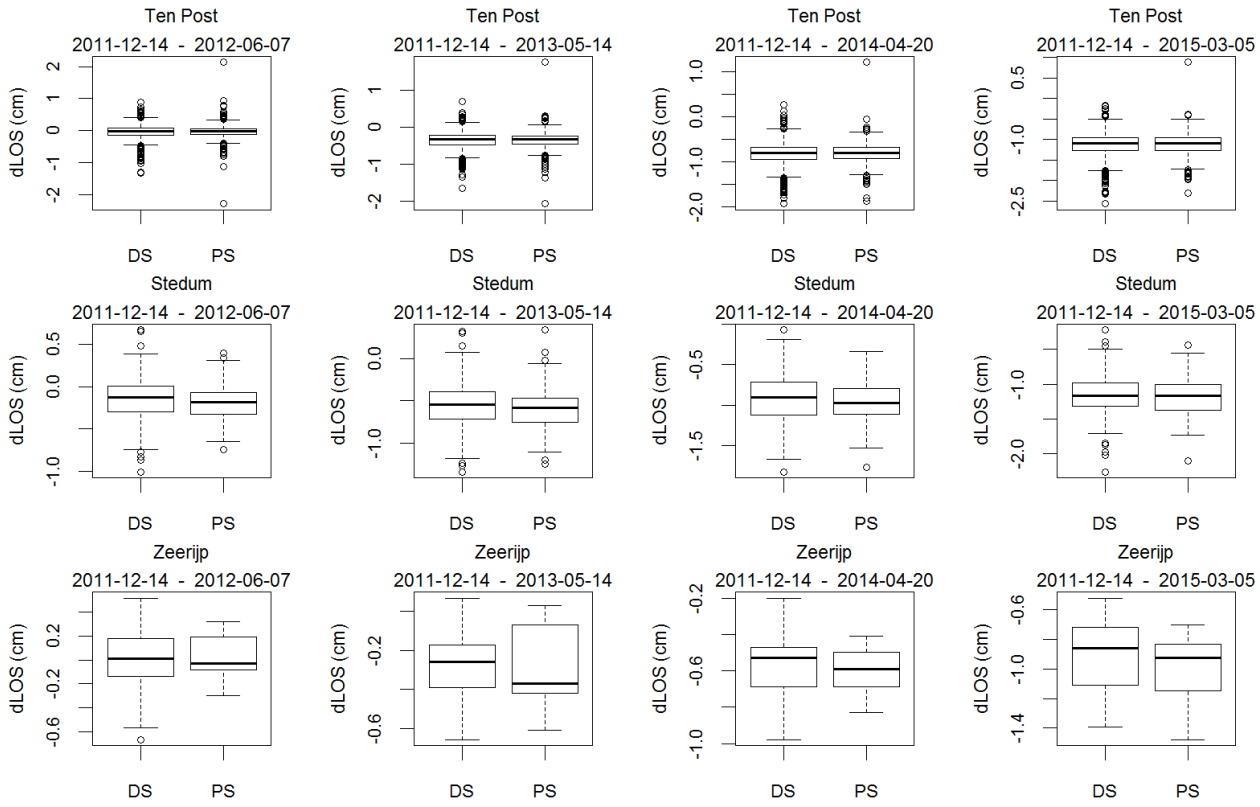

Figure 16: Boxplots of dLOS measurements from a sample of epochs, split accross PSs and DSs.

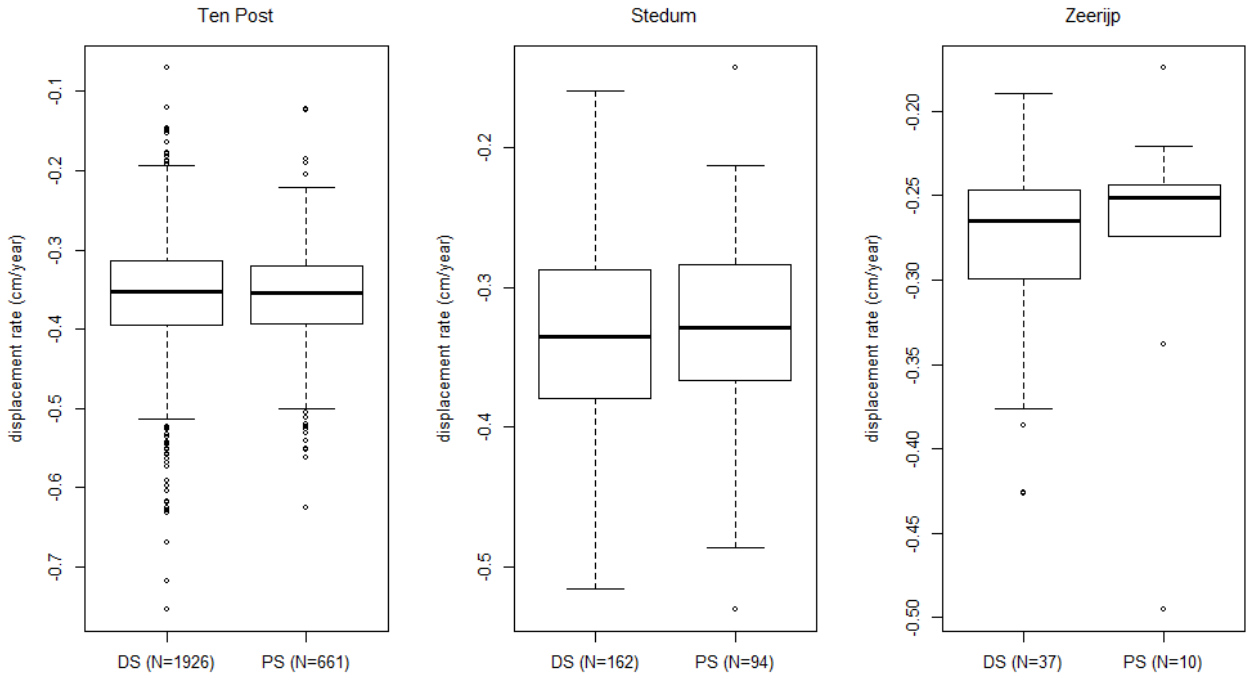

Figure 17: Boxplots of estimated linear trends in InSAR data, for PSs and DSs.

D Visual assessment of correspondence GPS and InSAR

Figure 18: Pictures of the permanent GPS stations at Stedum, Zeerijp and Ten Post. The stations at Stedum and Zeerijp have been attached to specially constructed monuments with foundations with depths of 22 and 28 meters respectively. The GPS receiver at Ten Post has been mounted to the side of a building.

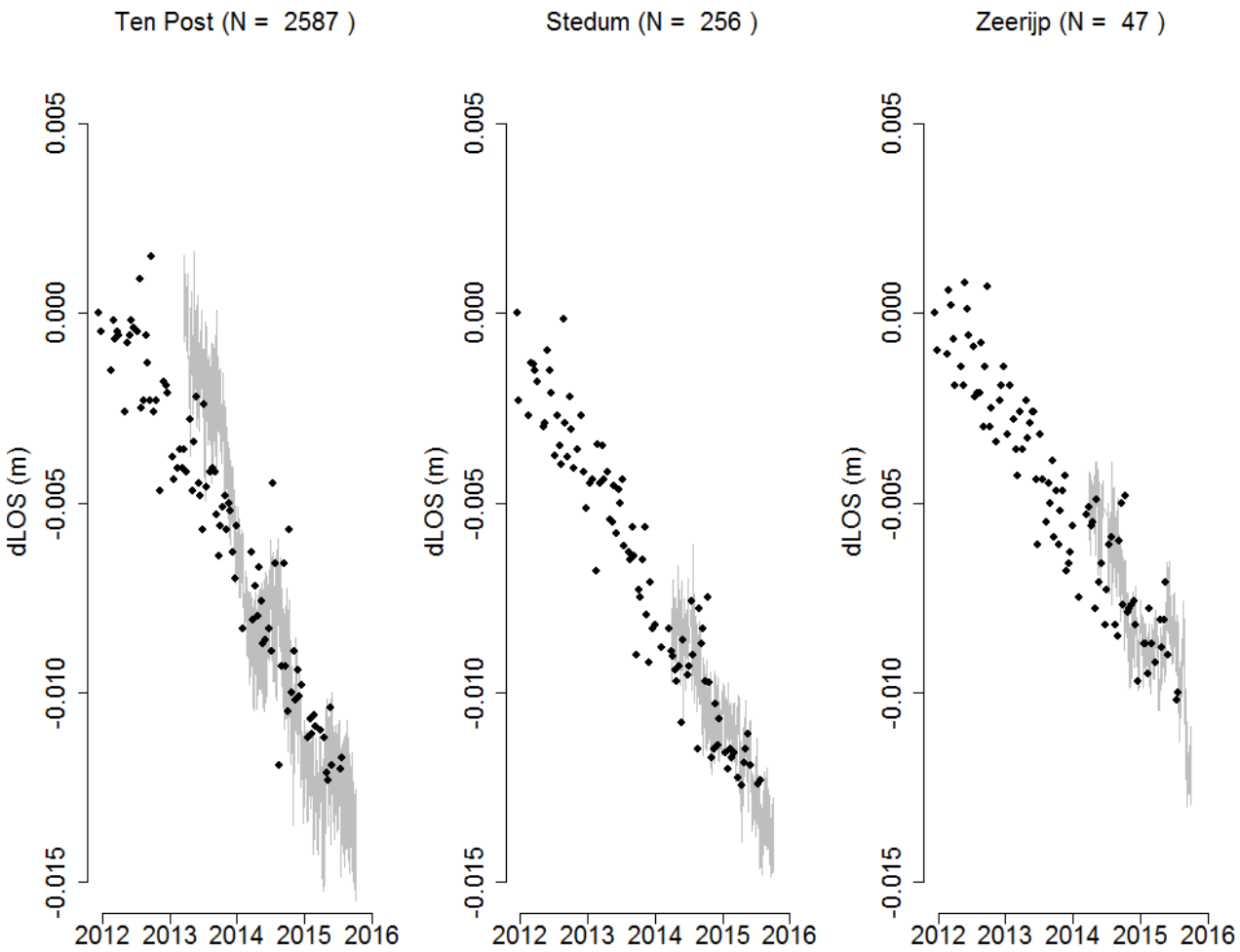

Figure 19: Filled dots: median dLOS from PS and DS InSAR. Grey lines: hourly dLOS from the GPS receiver. For ease of visual interpretation, the time series have been alligned by setting their means at the overlapping time period to be equal.

References

P. J. Rousseeuw F. R. Hampel, E. M. Ronchetti and W. A. Stahel. *Robust Statistics: The Approach Based on Influence Functions*. Wiley-Interscience paperback series. New York: John Wiley and Sons, 1986.

M. Frigge, D. C. Hoaglin, and B. Iglewicz. Some implementations of the boxplot. *The American Statistician*, 43:50–54, 1989.

Hastie and Tibshirani. *Generalized Additive Models*. Chapman and Hall, 1990.

NAM. Technical addendum to the winningsplan groningen 2013 subsidence, induced earthquakes and seismic hazard analysis in the groningen field. Technical report, NAM, 2013.

F. P. Pijpers. Phase 0 report 1: significance of trend changes in ground subsidence in groningen. *CBS 2014 Scientific Paper*, 2014.

F. P. Pijpers and D.J. van der Laan. Phase 1 update may 2015: trend changes in ground subsidence in groningen. *CBS 2015 Scientific Paper*, 2015.

R Core Team. *R: A Language and Environment for Statistical Computing*. R Foundation for Statistical Computing, Vienna, Austria, 2014. URL `http://www.R-project.org/`.

F. van den Heuvel and M. Schouten. Groningen deformation monitoring using vhr-insar: Initial processing report. Technical report, SkyGeo, 2015.

H. van der Marel. Gnss processing groningen fase 1. *Technische Universiteit Delft: Rapport voor Staatstoezicht op de Mijnen (SodM)*, 2015.

W. N. Venables and B. D. Ripley. *Modern Applied Statistics with S*. Springer, New York, fourth edition, 2002. URL `http://www.stats.ox.ac.uk/pub/MASS4`. ISBN 0-387-95457-0.

S. Williams. Description of gps uncertainties within the long term study on anomalous time-dependent subsidence. Technical report, (National Oceanographic Centre Liverpool): Report commissioned by NAM for the long term subsidence study on anomalous time-dependent subsidence., 2015.

S. N. Wood. *Generalized Additive Models: An Introduction with R. Chapman and Hall/CRC*. London: Chapman and Hall/CRC, 2006.

S.N. Wood. Fast stable restricted maximum likelihood and marginal likelihood estimation of semiparametric generalized linear models. *Journal of the Royal Statistical Society (B)*, 73:3–36, 2011.